

Trimacrocylic Arylamine and its Polycationic States†

Akihiro Ito,*^a Yuko Yamagishi,^a Koji Fukui,^a Syuuzi Inoue,^a Yasukazu Hirao,^b Ko Furukawa,^c Tatsuhiro Kato^d and Kazuyoshi Tanaka^{a,b}

Received (in XXX, XXX) 1st April 2008, Accepted 1st January 2008

First published on the web 1st January 2008

DOI: 10.1039/b000000x

A novel trimacrocylic arylamine was found to be accessible to the different spin-states by consecutive electrochemical or chemical oxidation.

Alternating *meta*-phenylene- and *para*-phenylene-linked oligoarylamines are considered as promising molecular parts for the molecule-based electronics due to their intriguing magnetic and electronic properties.^{1–6} From the magnetic view of point, *meta*-phenylene linker plays a role in ensuring the effective ferromagnetic interaction, while *para*-phenylene linker takes an important part in stabilizing the spin-containing aminium radical cations. Of the *meta-para* oligoarylamines prepared so far, the macrocyclic oligoarylamines are structurally defined and, therefore, we can employ them as the component pieces to prepare the two- and/or three-dimensionally structured oligoarylamines. The synthesis of tetraaza[1₄]*m,p,m,p*-cyclophane, the smallest macrocyclic oligoarylamines possessing the alternating *meta-para* linkage, has been reported independently at the same time by three groups (Fig. 1(a)).⁵ Expectedly, these molecules were oxidized into di(radical cation) with parallel spin-alignment. Moreover, recently, Hartwig and co-workers have succeeded in synthesizing the three- and four-runged ladder-type oligoarylamines (Fig. 1(b)).⁶ However, the ground state of the dicationic species was determined to be a spin-singlet, although the generated spins are of delocalized character.

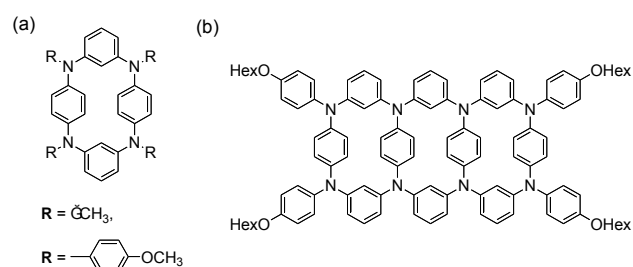
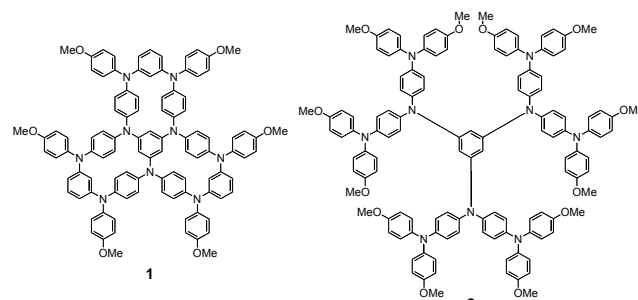


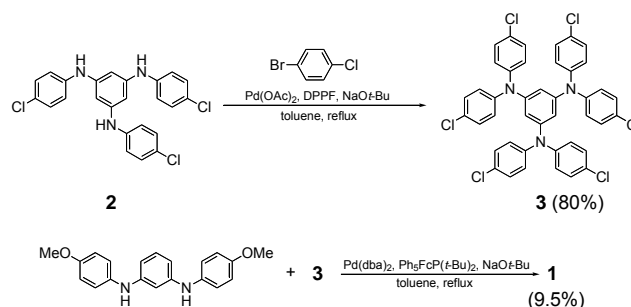
Fig. 1 (a) Tetraaza[1₄]*m,p,m,p*-cyclophane and (b) its extension to the ladder-type trimacrocycle

When the tetraazacyclophane structure in Fig. 1(a) is utilized as a building block for constructing the trimacrocylic oligoarylamine molecular system such as the ladder-type molecule in Fig. 1(b), there exists another option; the star-shaped extension. For the purpose of elucidating the electronic structures of polycationic species of the star-shaped trimacrocylic oligoarylamine, we synthesized a trimacrocycle **1**. The trimacrocycle **1** can also be regarded as an analog of the star-shaped oligoarylamine **2**. We have recently determined the spin multiplicities in tri(radical cation) of the



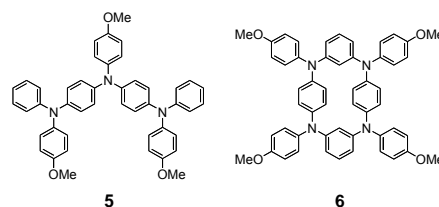
star-shaped oligoarylamine **2**.^{3c}

Palladium-catalyzed aryl amination reaction of 1,3,5-tris[di(4-chlorophenyl)amino]benzene (**3**) with 1,3-bis[(4-methoxyphenyl)amino]benzene (**4**) gives the trimacrocycle **1** in around 10% yield, in a one-pot reaction (Scheme 1, ESI†).



Scheme 1 Synthesis of trimacrocylic arylamine **1**.

Electrochemical oxidation of the trimacrocycle **1** by the cyclic voltammetry (CV) in CH₂Cl₂ exhibits five redox couples as shown in Fig. 2. All the oxidation processes are chemically reversible after repeated potential cycling in CH₂Cl₂. Judging from the differential pulse voltammogram (Fig. S1, ESI†), the first four oxidations are regarded as one-electron transfer process, while the fifth oxidation corresponds to quasi-two-electron transfer, indicating **1** is



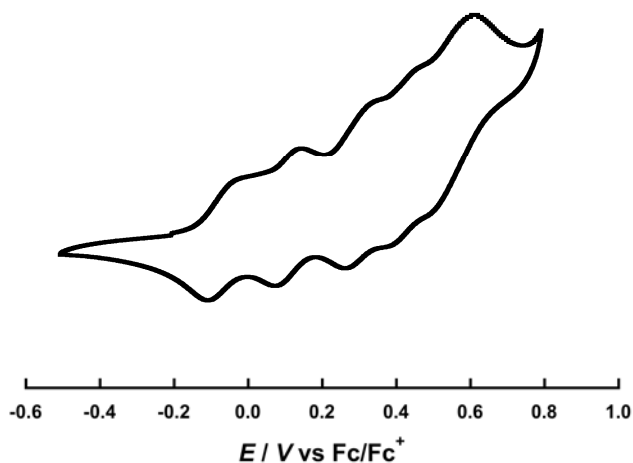
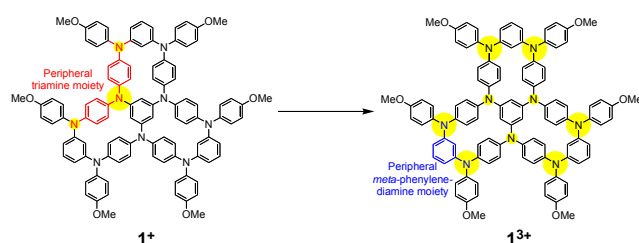
oxidizable up to hexacation. The oxidation potentials of **1** are summarized in Table 1 together with those of the related compounds under the same conditions.

Table 1 Oxidation potentials (in V) of **1** and the related compounds ^a

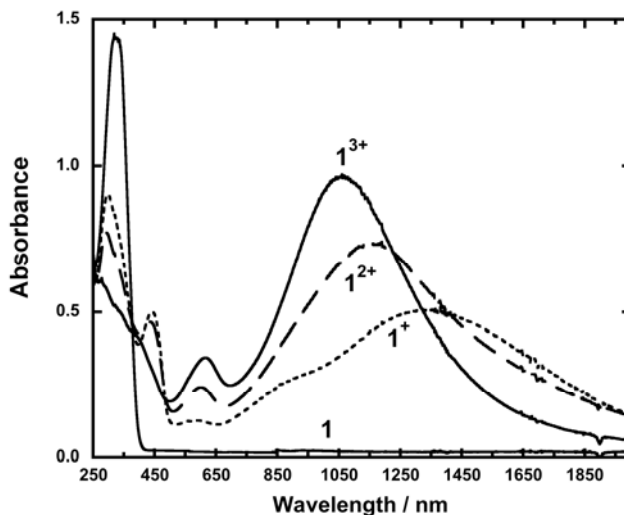
Compound	E_1	E_2	E_3	E_4	E_5
1	-0.12	0.09	0.28	0.41	0.53 ^b
2 ^c	-0.14	-0.01	0.09	0.19 ^d	—
5	-0.11	0.25	0.80 ^e	—	—
6	-0.01	0.22	0.54	0.67	—

^a 1 mM CH₂Cl₂ solution containing 0.1 M *n*-Bu₄NBF₄, potentials versus Fc/Fc⁺, Pt electrode, 298 K, scan rate 100 mV s⁻¹. ^b Quasi-two-electron transfer. ^c Measured in PhCN (see ref. 3(c)). ^d Quasi-three electron transfer. ^e Anodic peak potential (irreversible).

From the comparison of the oxidation potentials for **1** with those for the star-shaped analog **2**, the first three oxidations are assigned as one-electron removal from each peripheral triamine moiety. Each oxidation potential of **1** shifts to the higher value as compared with the corresponding value of **2**. This situation closely relates to the fact that all the nitrogen atoms are inevitably charged after the three-electron removal from **1**, and therefore, the electrostatic repulsion on the peripheral *meta*-phenylenediamine moieties cannot be ignored, as shown in Fig. 3.

**Fig. 2** Cyclic voltammograms of **1** measured in CH₂Cl₂ containing 0.1 M *n*-Bu₄NBF₄ at 298 K (scan rate 0.1 V s⁻¹).**Fig. 3** Schematic view of the charge distribution (yellow circles) in the charged states **1**⁺ and **1**³⁺.

We measured the optical absorption spectral changes of **1** in CH₂Cl₂ during the oxidation process of **1** to **1**³⁺ by using an optically transparent thin-layer electrochemical cell. As shown in Fig. 4, the lowest-energy absorption band at $\lambda_{\max} = 1336$ nm grew together with the shoulder band at ~ 900 nm upon oxidation of **1** to **1**⁺. Further oxidation to the dication **1**²⁺ resulted in blue shift and increase in intensity of the lowest-energy band ($\lambda_{\max} = 1154$ nm). Finally, in the resulting

**Fig. 4** Vis-NIR spectra of the stepwise electrochemical oxidation of **1** to **1**³⁺ in CH₂Cl₂/0.1 M *n*-Bu₄NBF₄ at room temperature: (a) **1**⁺ (dotted line), (b) **1**²⁺ (broken line), and (c) **1**³⁺ (solid line).

trication **1**³⁺, further blue shift and increase in intensity of the lowest energy band ($\lambda_{\max} = 1051$ nm) were observed. Note that the similar spectral change was also seen during the oxidation process of **5** to **5**²⁺ (Fig. S2). The spectral change in the charged states of **5** is expected to be influenced by the difference in charge distribution between **5**⁺ and **5**²⁺; the generated charge in **5**⁺ is considered to be distributed over the central triphenylamine moiety, whereas that in **5**²⁺ is localized mainly on the outer two triphenylamine moieties to avoid the electrostatic repulsion. Therefore, it is anticipated that the charge distribution in the charged states of **1** changes from the central 1,3,5-triaminobenzene moiety to the peripheral three *meta*-phenylenediamine moieties, on going from **1**⁺ to **1**³⁺ (Fig. 3). This speculation can be supported by the comparison of the oxidation potentials for **1** with those for the triamine moiety **5** (Table 1). The first oxidation potentials of both **1** and **5** show almost the same value, while the third oxidation potential of **1** is similar to the second oxidation potential of **5**.

To explore the spin state of the each oxidized state of **1**, we measured the continuous wave ESR (cw-ESR) spectra of **1**⁺, **1**²⁺, **1**³⁺ and **1**⁴⁺ in the rigid-glass.⁷ However, neither the definitive fine-structured spectra⁸ nor the forbidden resonance⁸ due to the existence of high-spin species were observed at 123 K (Fig. S3, ESI†).⁷

To overcome the difficulty in identifying the spin multiplicity of the high-spin components, we carried out the electron spin transient nutation (ESTN) measurements⁹ based on the pulsed ESR method (Figs. 5 and S4, ESI†). As shown in Fig. S4a (ESI†), the nutation frequency (18 MHz = $\omega_{\text{dication}} = \omega_{\text{doublet}}$) observed at the central field is ascribed to $|1/2, -1/2\rangle \leftrightarrow |1/2, +1/2\rangle$ transition of the spin-doublet **1**⁺. For the sample treated by 2 molar equiv of oxidant, the new signal with the nutation frequency of 22 MHz (= ω_{dication}) appeared, and this corresponds to the $|1, 0\rangle \leftrightarrow |1, \pm 1\rangle$ transition for spin-triplet state (Fig. 5a). The generated triplet species can be regarded as **1**²⁺. After oxidation of **1** with 3 molar equiv of oxidant, two new intense signals with the same nutation frequency of 33 MHz (= $\omega_{\text{trication}}$) were seen in

addition to that for the spin-triplet species ($\omega_{\text{dication}} = 24$ MHz) as impurities in the sample (Fig. 5b). From the frequency ratio ($\omega_{\text{trication}}/\omega_{\text{doublet}} \sim \sqrt{3}$), these nutation signals are assigned to the $|3/2, \pm 3/2\rangle \leftrightarrow |3/2, \pm 1/2\rangle$ transition for spin-quartet state, clearly indicating the dominance of spin-quartet $\mathbf{1}^{3+}$. Finally, when 4 molar equiv of oxidant is added, the observed nutation signals were detected at 25 MHz, corresponding to the generation of spin-triplet species on the basis of the frequency ratio ($\omega_{\text{tetracation}}/\omega_{\text{doublet}} \sim \sqrt{2}$) (Fig. S4b, ESI†). Considering the quantity of added oxidant, the observed triplet species is considered as $\mathbf{1}^{4+}$. This results suggests the newly generated spin is antiferromagnetically coupled to the existing three spins. As a whole, the consecutive oxidations of **1** lead to the charged states $\mathbf{1}^+$, $\mathbf{1}^{2+}$, $\mathbf{1}^{3+}$, and $\mathbf{1}^{4+}$ with doublet, triplet, quartet, and triplet spin multiplicities, respectively, at low temperature.

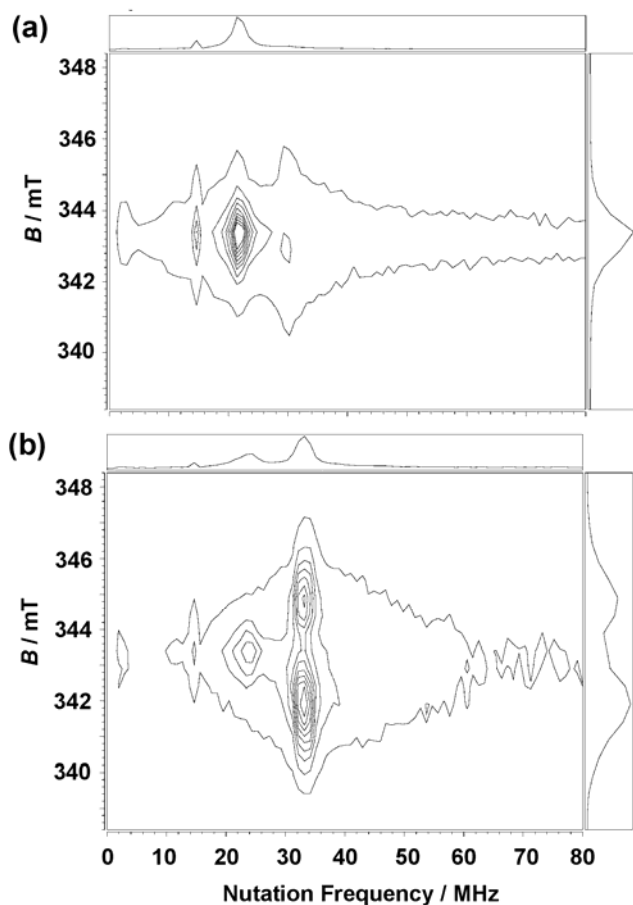


Fig. 5 2D ESR spectra of **1** in toluene/*n*-hexane at 5 K after the addition of (a) 2 equiv and (b) 3 equiv of oxidant.

In summary, we have prepared a novel trimacrocylic arylamine with a rigid molecular structure. From the electrochemical study, it was confirmed that this trimacrocycle is oxidizable up to the hexacation, and the chemically generated dication and trication are in high-spin triplet and quartet states, respectively, whereas the tetracation is in low-spin triplet state probably because of the partial antiferromagnetic coupling among four radical spins. The present polymacrocylic molecular spin system may open the possibility for its extension to a larger two-dimensional

molecular spin system.

The present work was supported by Grant-in-Aid for Scientific Research (B) (20350065) from the Japan Society for the Promotion of Science (JSPS) and from CREST (Core Research for Evolutional Science and Technology) of the Japan Science and Technology Agency (JST). Thanks are due to the Research Center for Molecular-Scale Nanoscience in the Institute for Molecular Science for the use of a pulsed ESR spectrometer.

Notes and references

- ^a Department of Molecular Engineering, Graduate School of Engineering, Kyoto University, Nishikyo-ku, Kyoto 615-8510, Japan. E-mail: aito@scl.kyoto-u.ac.jp
- ^b CREST, Japan Science and Technology Agency (JST), Japan
- ^c Institute for Molecular Science, Myodaiji, Okazaki 444-8585, Japan
- ^d Department of Chemistry, Josai University, 1-1 Keyakidai, Sakado, Saitama 350-0295, Japan
- † Electronic Supplementary Information (ESI) available: Experimental section and the electrochemical and spectroscopic data. See DOI: 10.1039/b000000x/
- (a) M. M. Wienk and R. A. J. Janssen, *Chem. Commun.*, 1996, 267; (b) M. M. Wienk and R. A. J. Janssen, *J. Am. Chem. Soc.*, 1996, **118**, 10626; (c) M. M. Wienk and R. A. J. Janssen, *J. Am. Chem. Soc.*, 1997, **119**, 4492; (d) M. P. Struijk and R. A. J. Janssen, *Synth. Met.*, 1999, **103**, 2287; (e) P. J. van Meurs and R. A. J. Janssen, *J. Org. Chem.*, 2000, **65**, 5712.
 - (a) K. R. Sticley, T. D. Selby and S. C. Blackstock, *J. Org. Chem.*, 1997, **62**, 448; (b) T. D. Selby and S. C. Blackstock, *J. Am. Chem. Soc.*, 1998, **120**, 12155; (c) T. D. Selby and S. C. Blackstock, *J. Am. Chem. Soc.*, 1999, **121**, 7152; (d) T. D. Selby, K. R. Sticley and S. C. Blackstock, *Org. Lett.* 2000, **2**, 171; (e) T. D. Selby, K.-Y. Kim and S. C. Blackstock, *Chem. Mater.*, 2002, **14**, 1685; (f) K.-Y. Kim, J. D. Hassenzahl, T. D. Selby, G. J. Szulczewski and S. C. Blackstock, *Chem. Mater.*, 2002, **14**, 1691; (g) J. C. Li, K.-Y. Kim, S. C. Blackstock and G. J. Szulczewski, *Chem. Mater.*, 2004, **16**, 4711.
 - (a) A. Ito, A. Taniguchi, T. Yamabe and K. Tanaka, *Org. Lett.*, 1999, **1**, 741; (b) A. Ito, H. Ino, Y. Matsui, Y. Hirao and K. Tanaka, *J. Phys. Chem. A*, 2004, **108**, 5715; (c) Y. Hirao, H. Ino, A. Ito, K. Tanaka and T. Kato, *J. Phys. Chem. A*, 2006, **110**, 4866; (d) Y. Hirao, A. Ito and K. Tanaka, *J. Phys. Chem. A*, 2007, **111**, 2951; (e) A. Ito, S. Inoue, Y. Hirao, K. Furukawa, T. Kato and K. Tanaka, *Chem. Commun.*, 2008, 3242.
 - (a) I. Kulszewicz-Bajer, M. Zagórska, I. Wielgus, M. Pawłowski, J. Gosk and A. Twardowski, *J. Phys. Chem. B*, 2007, **111**, 34; (b) I. Kulszewicz-Bajer, J. Gosk, M. Pawłowski, S. Gambarelli, D. Djurado and A. Twardowski, *J. Phys. Chem. B*, 2007, **111**, 9421; (c) M. Gątecka, I. Wielgus, M. Zagórska, M. Pawłowski and I. Kulszewicz-Bajer, *Macromolecules*, 2007, **40**, 4924.
 - (a) A. Ito, Y. Ono and K. Tanaka, *Angew. Chem. Int. Ed.*, 2000, **39**, 1072; (b) T. D. Selby and S. C. Blackstock, *Org. Lett.*, 1999, **1**, 2053; (c) S. I. Hauck, K. V. Lakshmi and J. F. Hartwig, *Org. Lett.*, 1999, **1**, 2057.
 - X. Z. Yan, J. Pawlas, T. Goodson, III and J. F. Hartwig, *J. Am. Chem. Soc.*, 2005, **127**, 9105.
 - The stepwise chemical oxidation with tris(4-bromophenyl)ammonium hexachloroantimonate (TBA•SbCl₆) at 195 K in toluene/*n*-butyronitrile (8:2 (v/v)) generated the corresponding radical cations $\mathbf{1}^+$ to $\mathbf{1}^{4+}$. Trimacrocycle **1** does not easily dissolve in polar solvents such as CH₂Cl₂, *n*-butyronitrile, and so forth, and thus, the measurements were executed only by using a dilute solution of toluene/*n*-butyronitrile. Therefore, we could not observe the forbidden $\Delta M_S = \pm 2$ resonance in a half-field region of the allowed $\Delta M_S = \pm 1$ resonance.
 - W. Weltner, Jr., *Magnetic Atoms and Molecules*, Dover, New York, 1989.

-
- 9 (a) J. Isoya, H. Kanda, J. R. Norris, J. Tang and M. K. Brown, *Phys. Rev. B*, 1990, **41**, 3905; (b) A. V. Astashkin and A. Schweiger, *Chem. Phys. Lett.*, 1990, **174**, 595.

Supplementary Information for:

Trimacrocylic Arylamine and its Polycationic States

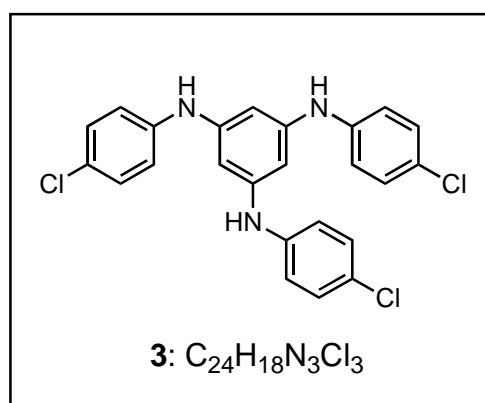
Akihiro Ito,^{*a} Yuko Yamagishi,^a Koji Fukui,^a Syuuzi Inoue,^a Yasukazu Hirao,^b Ko Furukawa,^c Tatsuhiisa Kato^d and Kazuyoshi Tanaka^{a,b}

^a Department of Molecular Engineering, Graduate School of Engineering, Kyoto University, Nishikyo-ku, Kyoto 615-8510, Japan. E-mail: aito@scl.kyoto-u.ac.jp

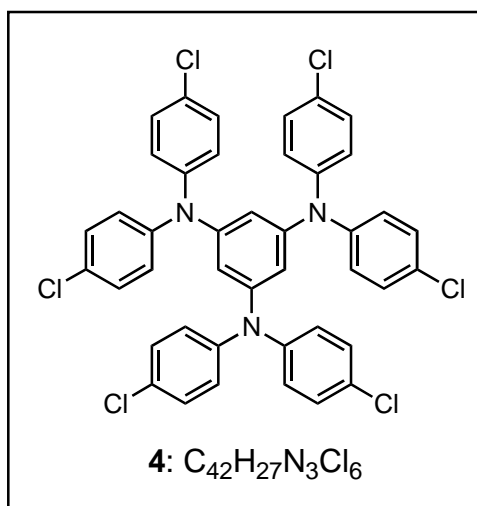
^b CREST, Japan Science and Technology Agency (JST), Japan

^c Institute for Molecular Science, Myodaiji, Okazaki 444-8585, Japan

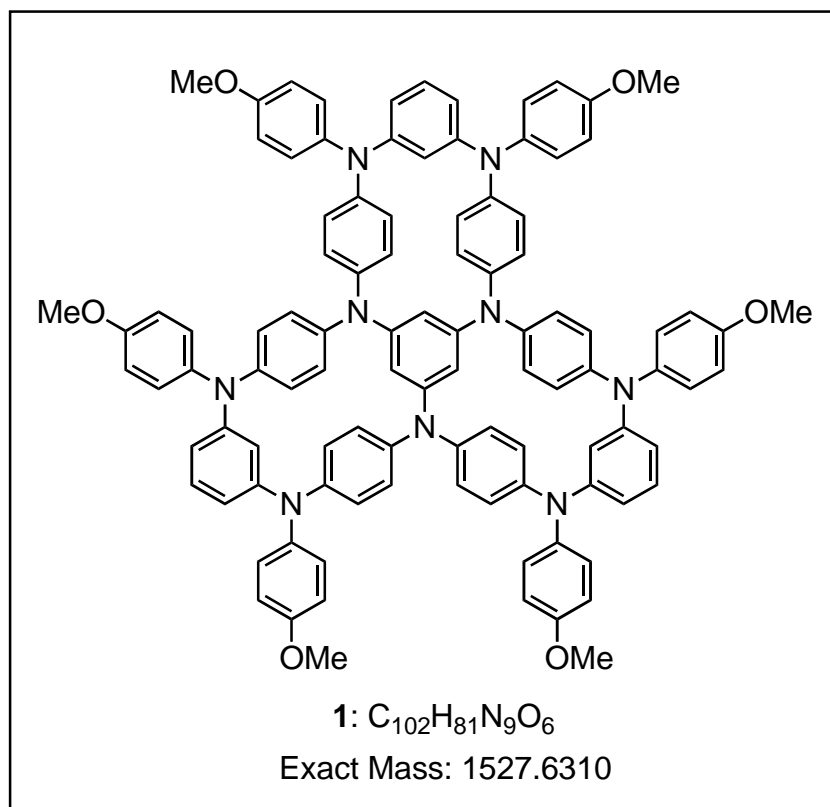
^d Department of Chemistry, Josai University, 1-1 Keyakidai, Sakado, Saitama 350-0295, Japan



***N,N',N''*-tris(4-chlorophenyl)-1,3,5-benzenetriamine (3).** To a mixture of phloroglucinol (1.26 g, 10.0 mmol), 4-chloroaniline (5.75 g, 45.1 mmol), and iodine (0.156 g, 0.6 mmol) was added toluene (5 ml) under argon atmosphere, and then the reaction mixture was refluxed with stirring for 29 h. After evaporation of the solvent, the residue was thoroughly washed with MeOH to afford **3** (3.87 g, 85%) as a purple solid: mp 232–234 °C; ¹H NMR (400 MHz, tetrahydrofuran-*d*₈) δ 7.29 (s, 3H), 7.14 (d, *J* = 8.8 Hz, 6H), 7.02 (d, *J* = 8.8 Hz, 6H), 6.32 (s, 3H); ¹³C NMR (100 MHz, tetrahydrofuran-*d*₈) δ 145.83, 143.60, 129.46, 124.76, 119.40, 100.05; EI HRMS (*m*-nitrobenzyl alcohol) *m/z* (relative intensity %) calcd for C₂₄H₁₈N₃O₃ [M]⁺ 453.0566, found 453.0569 (100).



***N,N,N',N',N'',N''*-hexakis(4-chlorophenyl)-1,3,5-benzenetriamine (4).** *p*-Bromochlorobenzene (8.63 g, 45.0 mmol), **3** (1.37 g, 3.00 mmol), NaOtBu (1.29 g, 13.5 mmol), Pd(OAc)₂ (34 mg, 0.15 mmol), and 1,1'-bis(diphenylphosphanyl)ferrocene (DPPF) (0.174 g, 0.30 mmol) were dissolved in toluene (30 ml) under argon atmosphere. The resulting solution was refluxed for 32 h with stirring. After evacuation of the solvent, CH₂Cl₂ and saturated aqueous solution of NaCl were added to the residue. The resulting organic layer was dried over MgSO₄, filtered, and concentrated. The residue was purified on column chromatography on silica gel using ethyl acetate / *n*-hexane (1:1 (v/v)), and was further recrystallized from ethyl acetate / *n*-hexane to yield **4** (1.89 g, 80%) as a white solid: mp 206–208 °C; ¹H NMR (400 MHz, C₆D₆) δ 6.90 (d, *J* = 8.8 Hz, 12H), 6.65 (d, *J* = 8.8 Hz, 12H), 6.96 (s, 2H), 6.86 (t, *J* = 6.0 Hz, 2H), 6.84 (d, *J* = 9.2 Hz, 16H), 6.78 (s, 2H), 6.78 (d, *J* = 8.7 Hz, 8H), 6.43 (s, 3H); ¹³C NMR (100 MHz, C₆D₆) δ 149.3, 145.3, 130.0, 129.1, 125.6, 113.0; EI HRMS (*m*-nitrobenzyl alcohol) *m/z* (relative intensity %) calcd for C₄₂H₂₇N₃O₆ [M]⁺ 783.0336, found 783.0336 (49.9).

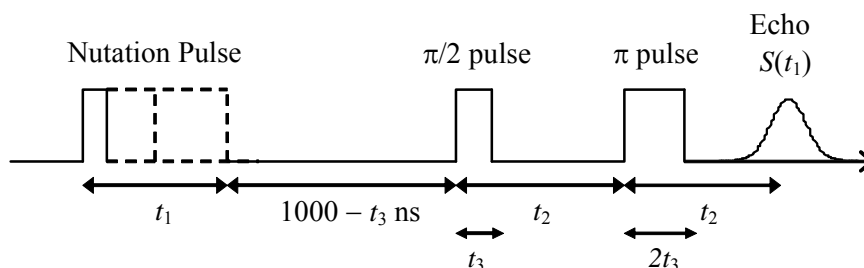


Trimacrocylic arylamine (1). Anhydrous toluene (8 ml) was added into a mixture of **4** (314 mg, 0.40 mmol), *N,N'*-bis(4-methoxyphenyl)-1,3-benzenediamine [**1**] (772 mg, 2.41 mmol), Pd(dba)₂ (13.7 mg, 0.024 mmol), Ph₅FcP(*t*-Bu)₂ [**2**] (29.4 mg, 0.041 mmol), and sodium *tert*-butoxide (1.07 g, 11.3 mmol) in a flask under argon, and the solution was heated to reflux for 16 h. After filtration through Celite, the filtrate was chromatographed on a silica gel (toluene/ethyl acetate = 2:1 as eluent), and recrystallization from toluene/*n*-hexane afforded **1** (58 mg, 9.5 %) as white powder: mp > 300 °C; ¹H NMR (400 MHz, tetrahydrofuran-*d*₈) δ 7.06 (d, *J* = 8.8 Hz, 12H), 7.03 (d, *J* = 8.8 Hz, 12H), 6.88 (m(=t+d), 3H+12H), 6.81 (d, *J* = 8.8 Hz, 12H), 6.38 (dd, *J* = 8.4, 2.0 Hz, 6H), 6.33 (d, *J* = 2.0 Hz, 3H), 5.62 (s, 3H), 3.73 (s, 18H); ¹³C NMR (100 MHz, tetrahydrofuran-*d*₈) δ 157.19, 150.46, 150.29, 144.74, 142.66, 140.83, 133.98, 129.76, 128.14, 127.64, 126.40, 115.24, 113.97, 102.14, 55.50; FAB HRMS (*m*-nitrobenzyl alcohol) *m/z* (relative intensity %) calcd for C₁₀₂H₈₁N₉O₆ [M]⁺ 1527.6310, found 1527.6316 (46.7).

[1] F. E. Goodson and J. F. Hartwig, *Macromolecules*, 1998, **31**, 1700.

[2](a) Q. Shelby, N. Kataoka, G. Mann and J. F. Hartwig, *J. Am. Chem. Soc.*, 2000, **122**, 10718; (b) N. Kataoka, Q. Shelby, J. P. Stambuli and J. F. Hartwig, *J. Org. Chem.*, 2002, **67**, 5553.

Pulsed ESR Measurements: The magnetic moments with distinct spin quantum numbers (S) precess with their specific nutation frequency (ω_n) in the presence of a microwave irradiation field and a static magnetic field. The nutation frequency for a transition from $|S, M_S\rangle$ to $|S, M_S+1\rangle$ can be expressed as $\omega_n = [S(S+1) - M_S(M_S+1)]^{1/2}\omega_0$ under certain conditions. This indicates that ω_n can be scaled with the total spin quantum number S and the spin magnetic quantum number M_S in the unit of ω_n ($= \omega_0$) for the doublet species; $\sqrt{2}$ for $S = 1$, $\sqrt{3}$ and 2 for $S = 3/2$. For determination of spin-multiplicity for high-spin molecules by using the pulsed ESR technique, see: (a) J. Isoya, H. Kanda, J. R. Norris, J. Tang and M. K. Brown, *Phys. Rev. B*, 1990, **41**, 3905; (b) A. V. Astashkin and A. Schweiger, *Chem. Phys. Lett.*, 1990, **174**, 595; (c) K. Sato, M. Yano, M. Furuichi, D. Shiomi, T. Takui, K. Abe, K. Itoh, A. Higuchi, K. Katsuma, Y. Shiota, *J. Am. Chem. Soc.*, 1997, **119**, 6607. (d) H. Bock, K. Gharagozloo-Hubmann, M. Sievert, T. Prisner and Z. Havlas, *Nature*, 2000, **404**, 267. (e) A. Ito, H. Ino, K. Tanaka, K. Kanemoto and T. Kato, *J. Org. Chem.*, 2002, **67**, 491.



Pulsed ESR measurements were carried out on a Bruker ELEXES E580 X-band FT ESR spectrometer. The ESTN measurements were performed by the three-pulse sequence shown below. The two-pulse ($\pi/2 - \pi$ pulses) electron spin-echo signal $S(t_1)$ was detected by increasing the width

(t_1) of the nutation pulse. The observed signal $S(t_1, B_0)$ as a function of external magnetic field B_0 is converted into a nutation frequency $S(\omega_n, B_0)$ spectrum. The parameters used for the measurements were $t_2 = 400$ ns, $t_3 = 8$ ns.

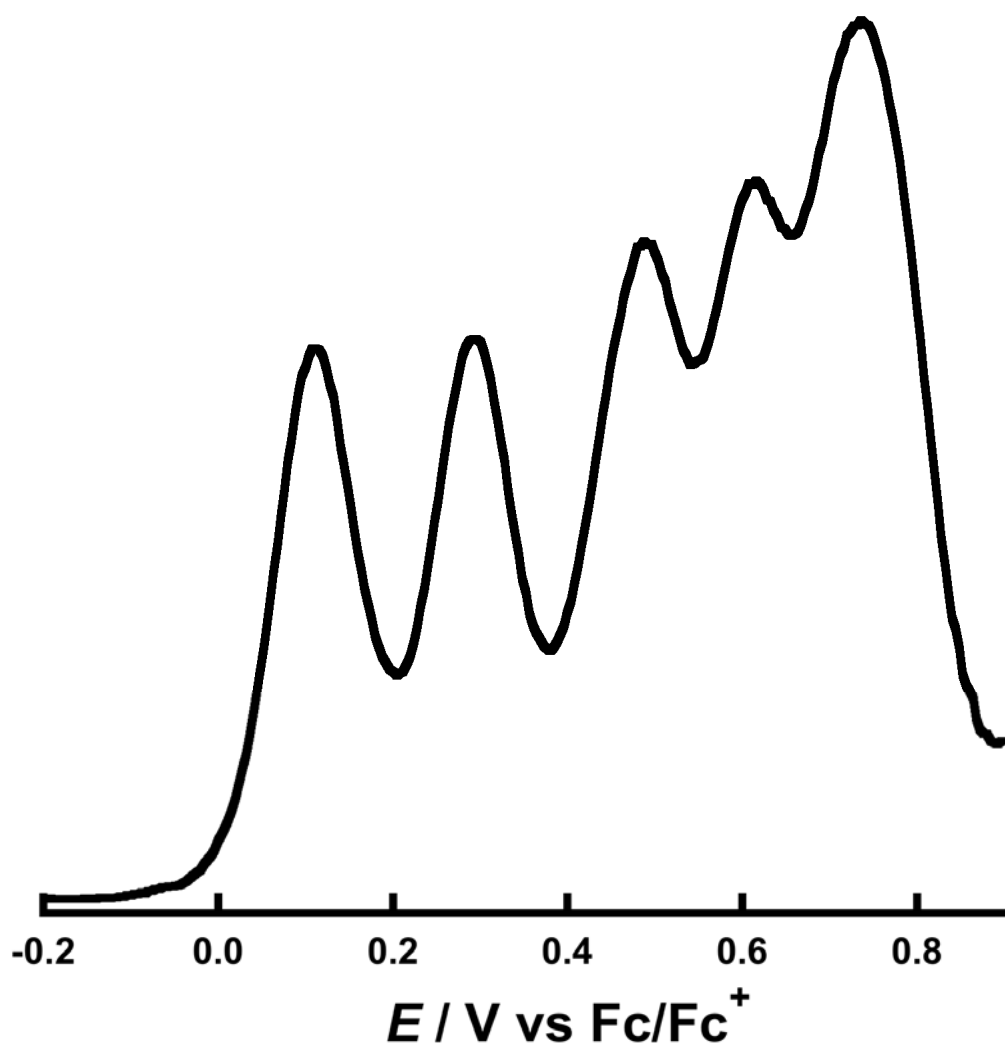


Fig. S1. Differential pulse voltammogram of **1** measured in CH_2Cl_2 containing 0.1 M $n\text{-Bu}_4\text{NBF}_4$ at 298 K (scan rate 0.1 V s^{-1}).

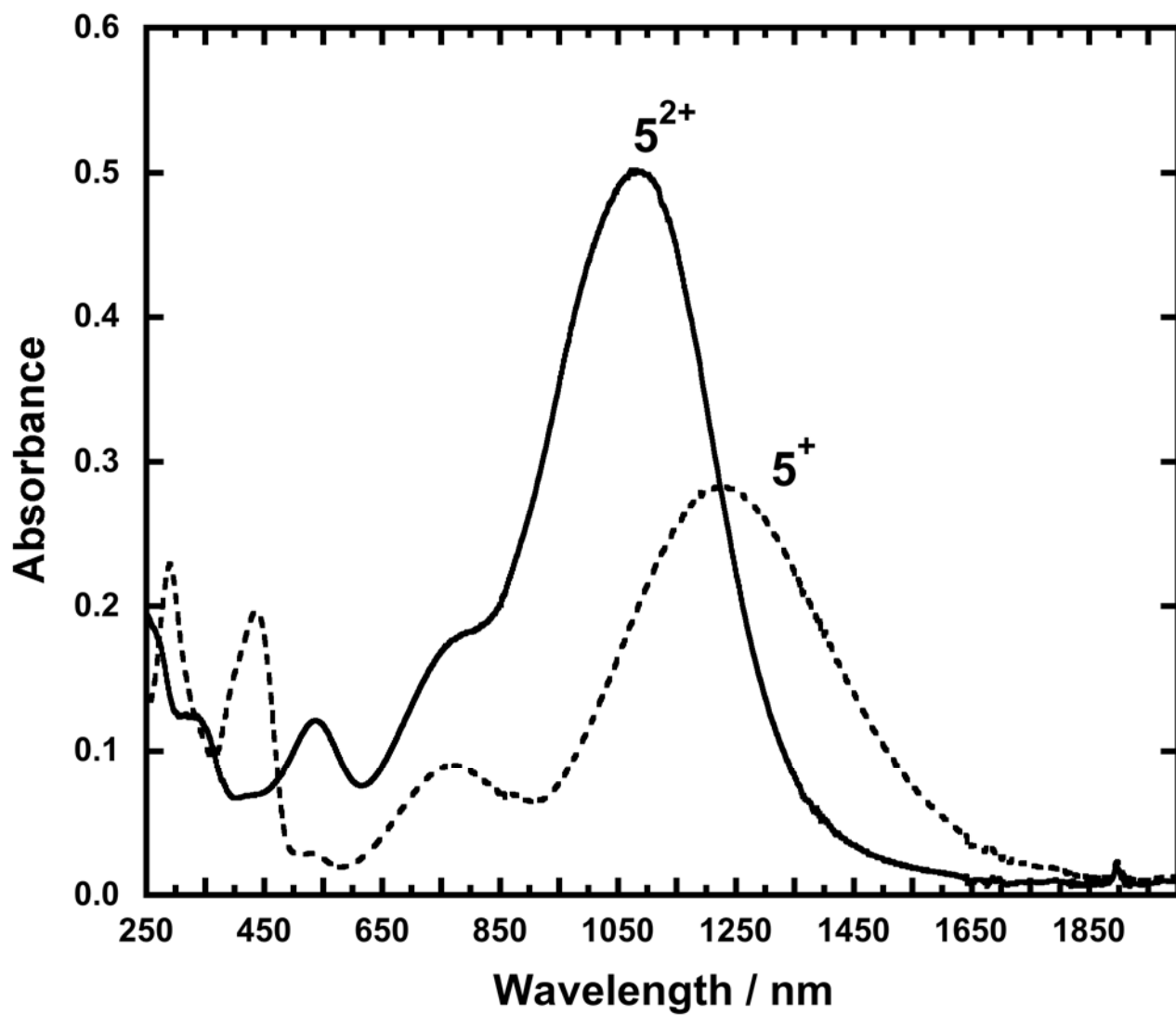


Fig. S2. Vis-NIR spectra during the stepwise electrochemical oxidation of **5** in $\text{CH}_2\text{Cl}_2/0.1\text{M}$ $n\text{-Bu}_4\text{NBF}_4$ at room temperature: 5^+ (dotted line) and 5^{2+} (solid line).

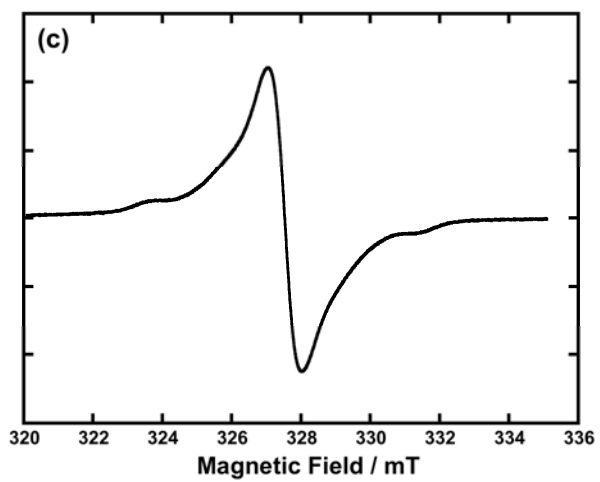
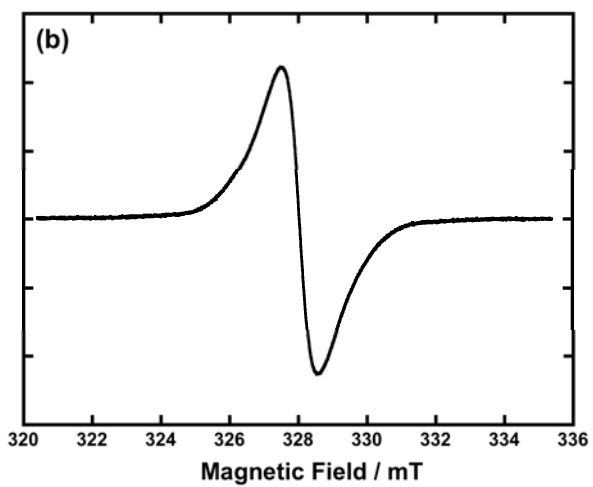
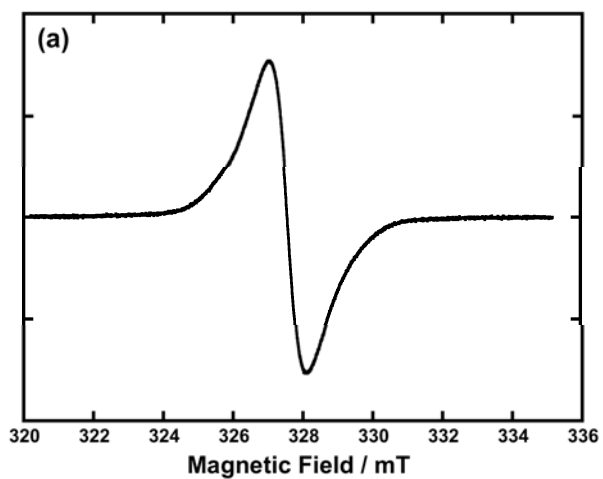


Fig. S3. CW-ESR spectra of **1** at 123 K after addition of (a) 1 equiv, (b) 2 equiv, and (c) 3 equiv of oxidant.

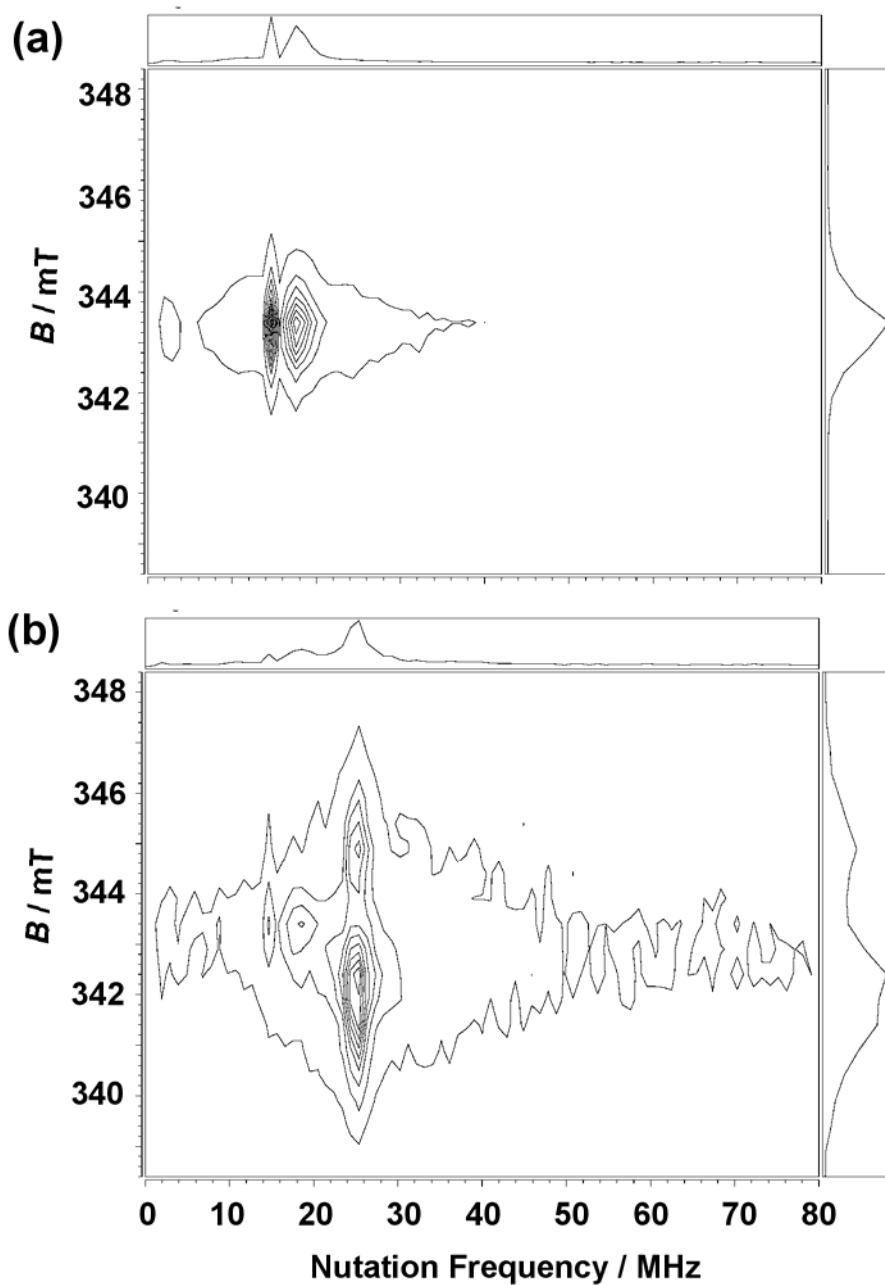


Fig. S4. 2D ESTN spectra of **1** in toluene/*n*-hexane (8:2 (v/v)) at 5 K after the addition of (a) 1 equiv and (b) 4 equiv of oxidant.